PHYSICAL REVIEW D **84,** 083007 (2011)

Cross-correlation search for a hot spot of gravitational waves

Sanjeev Dhurandhar,[1] Hideyuki Tagoshi,[2] Yuta Okada,[3] Nobuyuki Kanda,[3] and Hirotaka Takahashi[4,5]

[1]*Inter-University Centre for Astronomy and Astrophysics, Post Bag 4, Ganeshkhind, Pune 411007, India*
[2]*Department of Earth and Space Science, Graduate School of Science, Osaka University, Toyonaka, Osaka 560-0043, Japan*
[3]*Department of Physics, Graduate School of Science, Osaka City University, Sugimoto 3-3-138, Sumiyoshi-ku, Osaka 558-8585, Japan*
[4]*Department of Humanities, Yamanashi Eiwa College, 888, Yokone, Kofu, Yamanashi 400-8555, Japan*
[5]*Earthquake Research Institute, University of Tokyo, Bunkyo-Ku, Tokyo 113-0032, Japan*

(Received 27 May 2011; published 13 October 2011)

The cross-correlation search has been previously applied to map the gravitational wave (GW) stochastic background in the sky and also to target GW from rotating neutron stars/pulsars. Here we investigate how the cross-correlation method can be used to target a small region in the sky spanning at most a few pixels, where a pixel in the sky is determined by the diffraction limit which depends on the (i) baseline joining a pair of detectors and (ii) detector bandwidth. Here as one of the promising targets, we consider the Virgo cluster—a ''hot spot'' spanning few pixels—which could contain, as estimates suggest $\sim 10^{11}$ neutron stars, of which a small fraction would continuously emit GW in the bandwidth of the detectors. For the detector baselines, we consider advanced detector pairs among LCGT, LIGO, Virgo, ET, etc. Our results show that sufficient signal to noise can be accumulated with integration times of the order of a year if the ellipticity of neutron stars is larger than 10^{-6}. The results improve for the multibaseline search. This analysis could as well be applied to other likely hot spots in the sky and other possible pairs of detectors.

DOI: 10.1103/PhysRevD.84.083007 PACS numbers: 95.85.Sz, 04.80.Nn, 07.05.Kf, 95.55.Ym

I. INTRODUCTION

An enigmatic prediction of Einstein's general theory of relativity are gravitational waves (GWs). With the observed decay in the orbit of the Hulse-Taylor binary pulsar agreeing within a fraction of a percent with the theoretically computed decay from Einstein's theory, the existence of GWs was firmly established. Currently there is a worldwide effort to detect GWs with the operating interferometric gravitational wave observatories, the LIGO, Virgo, GEO and TAMA [1]. Now the advanced detectors being constructed include the upgraded LIGO and Virgo, the LCGT of Japan, LIGO-Australia and future possibilities such as Einstein Telescope (ET) [2].

Different types of GW sources have been predicted and may be directly observed by these advanced detectors in the near future (see [3] and references therein for recent reviews). These include the GWs from isolated sources such as the coalescence of compact binaries, the stellar core collapse followed by supernova explosion, gamma ray bursts, and rotating asymmetric neutron stars. Other sources are the stochastic GWs produced either in the early stage of our universe or by an abundance of unresolved astrophysical sources in the recent universe. In this paper, we investigate the stochastic GWs from astrophysical sources. In particular, we will address the problem of the targeted search of stochastic GWs from a small region in the sky, typically of linear size of a few degrees (few pixels—a pixel determined by the diffraction limit)—a ''hot spot''—, where there is likely to be an abundance of independent, unresolved GW sources continuously producing a relatively large stochastic background. Such a scenario seems feasible for the Virgo cluster, which could contain about 10^{11} neutron stars, the current estimate being $10^8 - 10^9$ per galaxy. Out of these neutron stars a small fraction of them could be rotating sufficiently rapidly emitting GWs in the advanced detector bandwidth of several 100 Hz to about 1 kHz. These could produce a reasonable signal-to-noise ratio (SNR) with an integration time of the order of an year. Thus, the GW source consists of spinning asymmetric neutron stars whose amplitudes and phases are randomly distributed. We will be thus dealing with a localized stochastic GW source. This is only one type of GW source, but there could be contributions from other sources such as supernovae with asymmetric core collapse, binary black hole mergers, low-mass X-ray binaries and hydrodynamical instabilities in neutron stars, or even GWs from astrophysical objects that we never knew existed. These will only in general (statistically) add to the SNR. The detectors we consider for this paper are advanced detectors such as the LIGO, Virgo, LCGT, ET, etc., which are expected to have sufficient sensitivity for detecting a hot spot.

The detection strategy of isotropic stochastic GW background was introduced in [4–7] based on the cross-correlation method. The cross-correlation method was extended to detect the anisotropic components of stochastic GW background in [8] for the two LIGO detectors' case, and in [9] for space-based detectors. The most relevant method to detect the GW hot spot is given in [10] (henceforth referred to as paper I), which is also generally known as the radiometric method. The idea is to cross-correlate data streams from two detectors with an appropriate time-delay, namely, the time-delay between arrival times of a GW wavefront from a specific direction $\hat{\mathbf{\Omega}}$. This choice of

time-delay allows the sampling of the same wavefront. As the detector baseline rotates with the earth, the time-delay between the data streams changes during the course of the day. The statistic targets a patch (pixel) in the sky around $\hat{\mathbf{\Omega}}$, its size being determined by the diffraction limit, namely, the inverse of the band-width divided by the light travel time along the baseline. This statistic in fact is a point estimate of the signal received from the given direction $\hat{\mathbf{\Omega}}$ and is most appropriate for observing a hot spot and could be made optimal by ''masking'' the rest of the sky if the hot spot emits a strong signal.

The GW strain amplitude for a rotating neutron star is proportional to the square of the frequency [11],

$$h \sim 4\pi^2 \alpha \frac{G}{c^4} \frac{\varepsilon I}{R} f^2, \tag{1}$$

where $\alpha \lesssim 1$ is the orientation factor, G is the Newton's gravitational constant, c the speed of light, ε is the ellipticity of the neutron star, I the moment of inertia, R the distance to the source and f the GW frequency. Since the cross-correlation statistic is quadratic in the strain amplitude, it scales as the fourth power of the frequency and therefore the main contribution to the SNR will tend to come from high frequency sources assuming that they are relatively abundant in the high frequency regime. Thus it is the population of millisecond neutron stars that we must primarily consider. We then estimate the millisecond neutron star population from the astrophysical information that is available and show that one can get an acceptable SNR, $\rho \sim 1$, for an integration of time of about an year. Using multiple baselines improves the SNR further. We find that among the current or near future baselines, the baseline of the two LIGOs and the baseline of LIGO Livingston and a LIGO like detector at the AIGO site stand out—they give dominant contribution to the SNR.

In Sec. II, we give a brief description of the cross-correlation method and the statistic and then derive an expression for the optimal SNR. In Sec. III we describe the distribution of pulsars and their populations. In Sec. IV, we state our results and discuss them in light of the astrophysical scenarios that are possible and the sensitivities of the future advanced detectors such as the ET. Section V is devoted to the summary and the discussion.

II. THE CROSS-CORRELATION STATISTIC FOR TARGETING A HOT SPOT

We refer to paper I for the detailed arguments involved in defining the cross-correlation statistic. Here we only furnish the salient steps. Since here we are interested in observing a hot spot, we will restrict our discussion to a point source. The full statistic, which we denote by S, is a weighted sum of elementary pieces ΔS_k, $k = 1, 2, \ldots n$ defined over time-segments $t_k - \Delta t/2 \le t \le t_k + \Delta t/2$ which are labeled by k. The full observation time is $T = n\Delta t$. The Δt is so chosen that it is much larger than the possible time-delay between the detectors (which must be less than about 40 ms for ground-based detectors) and much less than the time required for the orientation of the detectors to change appreciably and also on the time scale in which the noise is stationary. Current values of Δt used in the data analysis carried out by the relevant groups in the LIGO Science Collaboration (LSC) vary from 32 to 192 seconds. Let us consider a pair of detectors labeled by $I = 1, 2$, then the data in the I^{th} detector is given by $x_I(t) = h_I(t) + n_I(t)$, the signal $h_I(t)$ is added to the noise $n_I(t)$ in the I^{th} detector. For a point source in the direction $\hat{\mathbf{\Omega}}$, the ΔS_k also becomes a function of $\hat{\mathbf{\Omega}}$. It can be expressed easily in the Fourier domain,

$$\Delta S_k(\hat{\mathbf{\Omega}}) = \int_{-\infty}^{\infty} df \tilde{x}_1^*(t_k; f) \tilde{x}_2(t_k; f) \tilde{Q}(t_k, f, \hat{\mathbf{\Omega}}), \tag{2}$$

where the $\tilde{x}_I^*(t_k; f)$ are short-term Fourier transforms (SFT) defined only over the interval Δt around t_k, namely,

$$\tilde{x}_I(t_k; f) := \int_{t_k - \Delta t/2}^{t_k + \Delta t/2} dt' x_I(t') e^{-2\pi i f t'}. \tag{3}$$

The $Q(t_k, f, \hat{\mathbf{\Omega}})$ is a filter function chosen so that it optimizes the filter output. It also depends on the power spectrum of the GW source and the power spectral densities of the noises in each of the detectors. As discussed in paper I, in the general case it is a far more complicated object—a functional—but for the case of a point source, it reduces to a function of the direction $\hat{\mathbf{\Omega}}$. Even then it remains a functional of the signal power spectral density and the noise power spectral density (PSD). With a slight abuse of notation we still write it as a function of f.

The ΔS_k are random variables because of the noise and for different k we take them to be uncorrelated. The mean and the variance of ΔS_k are denoted, respectively, by $\mu_k = \langle \Delta S_k \rangle$ and $\sigma_k^2 = \langle \Delta S_k^2 \rangle - \langle \Delta S_k \rangle^2$. It has been shown in paper I that the linear combination that yields the maximum SNR is

$$S = \frac{\sum_{k=1}^n \mu_k \sigma_k^{-2} \Delta S_k}{\sum_{k=1}^n \mu_k \sigma_k^{-2}}, \tag{4}$$

$$\rho = \left\{ \sum_{k=1}^n \mu_k^2 / \sigma_k^2 \right\}^{1/2}, \tag{5}$$

where ρ is the SNR. The sum over k can be converted into an integral over t and henceforth in this article we drop the suffix k and replace t_k by just t. This helps to avoid clutter without jeopardizing clarity.

We now turn to the noise and signal PSDs in terms of which the SNR can be finally expressed. The signal cross-correlation in the two detectors in the limit of large time segment can be written as:

$$\langle \tilde{h}_1^*(t, f) \tilde{h}_2(t, f') \rangle = \delta(f - f') H(f) \gamma(t, f, \hat{\mathbf{\Omega}}), \tag{6}$$

where $\gamma(t, f, \hat{\mathbf{\Omega}})$ is the so-called directed overlap reduction function analogous to the one defined in [5] for the full sky, and given in the case of the point source by

$$\gamma(t, f, \hat{\mathbf{\Omega}}) = \Gamma(\hat{\mathbf{\Omega}}, t) e^{2\pi i f \hat{\mathbf{\Omega}} \cdot \mathbf{\Delta x}(t)/c}, \tag{7}$$

$$\Gamma(\hat{\mathbf{\Omega}}, t) = F_{+1}(\hat{\mathbf{\Omega}}, t) F_{+2}(\hat{\mathbf{\Omega}}, t) + F_{\times 1}(\hat{\mathbf{\Omega}}, t) F_{\times 2}(\hat{\mathbf{\Omega}}, t), \tag{8}$$

and where the $\mathbf{\Delta x}(t)$ is the vector joining detector 1 to detector 2 and rotates with the Earth tracing out a cone. The F_{+I}, $F_{\times I}$, $I = 1, 2$, are the antenna pattern functions for the two detectors and for the two polarizations. As mentioned in paper I the directed overlap reduction function has a bandwidth of about 750 Hz as compared to the few tens of Hz for the overlap reduction function found by integrating over the full sky. This is the main advantage of this method in which the sensitive region of the detector bandwidth is sampled by the statistic. Further the quantity $f^2 H(f)$ is essentially the flux per unit frequency per unit solid angle. For the noise, we take the noise in the two detectors to be uncorrelated, $\langle n_1(t) n_2(t') \rangle = 0$, and the one-sided noise PSD in each detector I is given through the defining equation,

$$\langle \tilde{n}_I^*(t; f) \tilde{n}_I(t; f') \rangle = \frac{1}{2} \delta(f - f') P_I(t; |f|). \tag{9}$$

We also assume $\langle h_I(f) n_J(f') \rangle = 0$, $I, J = 1, 2$, that is the signal and noise are uncorrelated. We are now ready to write down the optimal filter. In paper I it has been shown that the optimal filter for a given time segment labeled by t and for a point source in the direction $\hat{\mathbf{\Omega}}$ is given by

$$Q(t, f, \hat{\mathbf{\Omega}}) = \lambda(t) \frac{H(f) \gamma^*(t, f, \hat{\mathbf{\Omega}})}{P_1(t; |f|) P_2(t; |f|)}, \tag{10}$$

where $\lambda(t)$ is a normalization constant, which in any case cancels out in the SNR. The SNR ρ is given in terms of $\mu(t)$ and $\sigma(t)$ which are the mean and standard deviation, respectively, of $\Delta S(t)$. To keep the expressions simple we assume that the noise in the detectors is stationary. This certainly will not be the case, but since we are only interested in order of magnitude results, the assumption is not unjustified. Then P_I becomes a function of f only. Also we consider a bandwidth $f_1 \le f \le f_2$ for evaluating the SNR; the lower limit f_1 is determined by the seismic cutoff, while the upper limit f_2 is decided by the GW sources above which we do not expect significant contribution to the SNR. Given this, the relevant quantities can be best expressed in terms of the following two averages:

$$\langle H^2 \rangle_{\rm BW} = \frac{2}{\Delta f} \int_{f_1}^{f_2} df \frac{H^2(f)}{P_1(f) P_2(f)}, \tag{11}$$

$$\langle \Gamma^2 \rangle_{\rm 1day}(\hat{\mathbf{\Omega}}) = \frac{1}{T_{\rm 1day}} \int_0^{T_{\rm 1day}} \Gamma^2(\hat{\mathbf{\Omega}}, t) dt, \tag{12}$$

TABLE I. The values of the square root of the one day (sidereal) average of Γ^2 are given for the Virgo cluster whose declination is $\sim +12.7°$ (the RA is irrelevant since we take a one day average). LIGO-L stands for LIGO-Livingston and LIGO-H for LIGO-Hanford.

$\langle \Gamma^2_{(V)} \rangle^{1/2}_{\rm 1day}$	LIGO-H	Virgo	LCGT	AIGO
LIGO-L	0.387	0.288	0.224	0.452
LIGO-H	...	0.214	0.215	0.312
Virgo	...	...	0.276	0.286
LCGT	...	...	...	0.256

where $\Delta f = f_2 - f_1$. The first is the noise weighted average of the signal $H^2(f)$, the suffix BW denotes bandwidth, while the second is the time average of the squared directed overlap reduction function taken over one sidereal day. It is a function of sky position of the source. But since the azimuth is averaged over 2π, it is just a function of the declination of the source. Then in terms of these averages we have,

$$\mu(t) = \lambda(\Delta t \Delta f) \langle H^2 \rangle_{\rm BW} \Gamma^2(\hat{\mathbf{\Omega}}, t), \tag{13}$$

$$\sigma(t) = \frac{1}{2} \lambda (\Delta t \Delta f)^{1/2} \langle H^2 \rangle^{1/2}_{\rm BW} \Gamma(\hat{\mathbf{\Omega}}, t). \tag{14}$$

Then using the continuous limit of Eq. (5), we may write the SNR ρ in terms of the averages as follows:

$$\begin{aligned} \rho &= \left[\frac{1}{\Delta t} \int_0^T dt \frac{\mu^2(t)}{\sigma^2(t)} \right]^{1/2}, \\ &= 2 (T \Delta f)^{1/2} \langle H^2 \rangle^{1/2}_{\rm BW} \langle \Gamma^2 \rangle^{1/2}_{\rm 1day}. \end{aligned} \tag{15}$$

We now use this expression to compute the SNR for the continuous wave sources from the Virgo cluster. We observe that the SNR scales as $\sqrt{T}$.

To fix ideas we can look at a simplified situation of identical detectors with white noise $P_I(f) = P_0$ in the frequency range $f_1 \le f \le f_2$ and $P_I = \infty$ otherwise. Similarly we may consider flat signal spectrum $H(f) = H_0$, then the SNR simplifies to

$$\rho = 2 [T \Delta f]^{1/2} \frac{H_0}{P_0} \langle \Gamma^2 \rangle^{1/2}_{\rm 1day}. \tag{16}$$

The values of $\langle \Gamma^2 \rangle^{1/2}_{\rm 1day}(\hat{\mathbf{\Omega}}_{(V)})$ which we write in short as $\langle \Gamma^2_{(V)} \rangle^{1/2}_{\rm 1day}$ for various combinations of detector baselines are given in Table I for the direction $\hat{\mathbf{\Omega}}_{(V)}$ of the Virgo cluster. The declination of the Virgo cluster is $\sim +12.7°$.

III. PULSAR POPULATION AND DISTRIBUTION

We consider gravitational waves from rotating neutron stars in the Virgo cluster. An important parameter of this source is the population of such neutron stars. The number of Galactic neutron stars is estimated to be $10^8 - 10^9$ since

the birth rate is about 10^{-2}/yr and the age of the Galactic disk is about 10^{10} yr. What is more important in our case is the number of Galactic neutron stars whose rotation period is of the order of milliseconds. From the survey of radio pulsars in our Galactic disk, the population of millisecond pulsars is estimated to be at least 40000 [12–14] which implies a birth rate of 2.9×10^{-6}/yr. This is consistent with other studies of the millisecond pulsar population by Ferrario and Wickramasinghe (3.2×10^{-6}/yr) [15] and by Story *et al.* ($4 - 5 \times 10^{-6}$/yr) [16]. From the recent observation of gamma rays with the Fermi satellite [17], the population of millisecond pulsars in our Galactic globular cluster is estimated to be 2600–4700, which is one order lower than millisecond pulsars in the Galactic disk. Although there might be significant population of millisecond pulsars which do not emit radio waves, X and gamma rays now, since the lifetimes of millisecond pulsars are believed to be long ($\sim 10^{10}$ yr) [18], we do not expect a large population of such millisecond pulsars to exist. Thus we adopt 40000 as a typical number of neutron stars per galaxy whose rotation period is of the order of milliseconds.

A catalog of radio pulsars is given in the ATNF pulsar database [19]. The distribution of observed radio pulsars is given in Fig. 1. We find that the distribution naturally falls into two regions separated by 50 Hz. In each region, the distribution is approximately Gaussian as seen from the figure. This means that the distributions in each region may be approximated as log-normal distributions given by:

$$P_1(\log f_r)d(\log f_r) = \frac{1}{\sqrt{2\pi}\sigma_1} e^{-((\log f_r - \log\mu_1)^2/2\sigma_1^2)} d(\log f_r), \quad (\text{for } f_r > 50 \text{ Hz}), \tag{17}$$

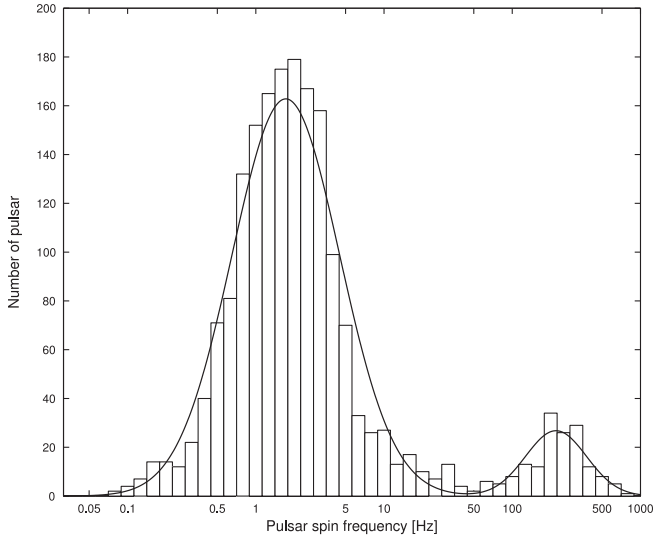

FIG. 1. The distribution of observed radio pulsars. The horizontal axis is $\log(f_r)$ where f_r is the rotational frequency of pulsars. The histogram is the observed number. The solid line is the two component Gaussian model of the distribution.

$$P_2(\log f_r)d(\log f_r) = \frac{1}{\sqrt{2\pi}\sigma_2} e^{-((\log f_r - \log\mu_2)^2/2\sigma_2^2)} d(\log f_r), \quad (\text{for } f_r < 50 \text{ Hz}), \tag{18}$$

where $\mu_1 = 219$ Hz, $\sigma_1 = 0.238$, $\mu_2 = 1.71$ Hz and $\sigma_2 = 0.420$, and $f_r = f/2$ (f is the gravitational wave frequency). P_1 and P_2 are normalized to unity when integrated from $f_r = 0$ to infinity.

The above observed distribution of pulsars is affected by selection effects and may not match with the true distribution. However, in this paper, we are interested only in the possibility of detecting the Virgo cluster hot spot. For this purpose, as a first step, we assume a similar bimodal form of distribution of neutron stars in the Virgo cluster. We assume that the total number of neutron stars in our Galaxy is 10^8 for $f_r < 50$ Hz, and 40000 for $f_r > 50$ Hz. Since there are approximately 10^3 galaxies in the Virgo cluster, the total number of neutron stars in the Virgo cluster is $N_{\text{low}} \sim 10^{11}$ for $f_r < 50$ Hz, $N_{\text{high}} \sim 4 \times 10^7$ for $f_r > 50$ Hz. The distribution of neutron stars including millisecond pulsars in Virgo cluster thus becomes

$$N(f)df = (N_{\text{high}}P_1(\log f_r) + N_{\text{low}}P_2(\log f_r))\frac{df_r}{f_r \ln 10}. \tag{19}$$

Since the length of data of one time-segment, Δt is at most 10^3 seconds, the frequency resolution is larger than 10^{-3} Hz. The frequency bandwidth can be taken as 10^3 Hz. Thus the number of frequency bins is 10^6. Since the number of pulsars with $f > 100$ Hz is 10^7, the number of pulsars in each frequency bin is about 10. In the low frequency regime this number is much larger. Thus, it is not possible to resolve the signal from each pulsar, which confirms the stochastic nature of the Virgo cluster hot spot.

IV. RESULTS

The spectral density of gravitational radiation from neutron stars in Virgo cluster, $H(f)$ is given as

$$H(f) = \langle h^2 \rangle N(f) = \left[7.05 \times 10^{-34}\left(\frac{\varepsilon}{10^{-5}}\right)\left(\frac{I}{1.1 \times 10^{45}\ \text{gcm}^2}\right)\right]^2 \times \langle \alpha^2 \rangle f^4 N(f)[\text{Hz}^{-1}], \tag{20}$$

where $\langle \alpha^2 \rangle$ represents the average with respect to the inclination angle and the polarization angle. Assuming uniform distribution of the sources over the angles, we have $\langle \alpha^2 \rangle = 0.4$. We also used the distance $R = 16.5$ Mpc.

In order to obtain a rough idea of how large $H(f)$ is compared with the noise power spectral density, it is convenient to define an effective source power, $H_{\text{eff}}(f)$ by,

$$H^2_{\rm eff}(f) = 8T_{\rm obs}\langle\Gamma^2\rangle_{\rm 1day} f H^2(f), \tag{21}$$

where $T_{\rm obs}$ is the observation time.

Then the signal-to-noise ratio is given by

$$\rho = \left[\int_{f_1}^{f_2} \frac{df}{f}\,\frac{H^2_{\rm eff}(f)}{P_1(f)P_2(f)}\right]^{1/2}. \tag{22}$$

The noise power spectral density of various advanced detectors including Einstein Telescope, as well as $H_{\rm eff}(f)$ are plotted in Fig. 2. Here, we assume $T_{\rm obs} = 1$ yr and $\langle\Gamma^2\rangle^{1/2}_{\rm 1day} = 0.2$. In this plot, $H_{\rm eff}(f)$ is plotted for $\varepsilon = 10^{-5}$, 10^{-6}, 10^{-7}. Although in these plots, we include the contribution from low frequency neutron stars with $f_r < 50$ Hz, the contribution of these to the SNR is very small, only about a few percent.

We now consider the quantity $\langle H^2\rangle^{1/2}_{\rm BW}\Delta f^{1/2}$. We find that

$$\langle H^2\rangle^{1/2}_{\rm BW}\Delta f^{1/2} \propto \left(\frac{\varepsilon}{10^{-5}}\right)^2\left(\frac{I}{1.1\times10^{45}\ {\rm gcm}^2}\right)^2\left(\frac{N_{\rm msp}}{4\times10^7}\right), \tag{23}$$

where $N_{\rm msp}$ is the number of millisecond pulsars. In general we write the signal-to-noise (SNR) for general direction $\hat{\mathbf{\Omega}}$ for a given baseline in terms of the SNR for the direction of the Virgo cluster. The SNR for 1 year observation for a general direction $\hat{\mathbf{\Omega}}$ is written as,

$$\rho(\hat{\mathbf{\Omega}}) = \rho_{(V)1\ \rm yr}\sqrt{\frac{T_{\rm obs}}{1\ \rm yr}}\left(\frac{\langle\Gamma^2\rangle^{1/2}_{\rm 1day}(\hat{\mathbf{\Omega}})}{\langle\Gamma^2_{(V)}\rangle^{1/2}_{\rm 1day}}\right)\left(\frac{\varepsilon}{10^{-5}}\right)^2 \times\left(\frac{I}{1.1\times10^{45}\ {\rm gcm}^2}\right)^2\left(\frac{N_{\rm msp}}{4\times10^7}\right), \tag{24}$$

where $\rho_{(V)1\ \rm yr}$ is the SNR for an observation period of 1 year and pertaining to the direction of the Virgo cluster. We now compute the observation time required to achieve $\rho = 3$ for a general direction $\hat{\mathbf{\Omega}}$, which we denote by $T^{\rho=3}_{\rm obs}(\hat{\mathbf{\Omega}})$. We choose $\rho = 3$ because the noise in the statistic $S(\hat{\mathbf{\Omega}})$, as argued in paper I, is distributed as a Gaussian with mean μ_S and standard deviation σ_S. This is the consequence of the generalized central limit theorem. The ρ is μ_S/σ_S. When no signal is present, we have, $\mu_S = 0$. Thus when we take $\rho > 3$, there is a more than 99.7% chance that the noise is not masquerading as the signal. We then have the following result:

$$T_{\rm obs}(\hat{\mathbf{\Omega}}) = T^{\rho=3}_{(V)\rm obs}\left(\frac{\langle\Gamma^2\rangle^{1/2}_{\rm 1day}(\hat{\mathbf{\Omega}})}{\langle\Gamma^2_{(V)}\rangle^{1/2}_{\rm 1day}}\right)^{-2}\left(\frac{\varepsilon}{10^{-5}}\right)^{-4} \times\left(\frac{I}{1.1\times10^{45}\ {\rm gcm}^2}\right)^{-4}\left(\frac{N_{\rm msp}}{4\times10^7}\right)^{-2}\left(\frac{\rho}{3}\right)^2, \tag{25}$$

where $T^{\rho=3}_{(V)\rm obs}$ is the corresponding observation time pertaining to the Virgo cluster.

In Tables I and II, the values of $\rho_{(V)1\ \rm yr}$ and $T^{\rho=3}_{(V)\rm obs}$ are tabulated for various detector baselines of advanced detectors. These tables may be used along with Eqs. (24) and (25) to obtain $\rho(\hat{\mathbf{\Omega}})$ and $T_{\rm obs}(\hat{\mathbf{\Omega}})$ for an arbitrary direction $\hat{\mathbf{\Omega}}$. In these tables, the noise PSD of AIGO is assumed to be the same as that of advanced LIGO. Further, since nothing

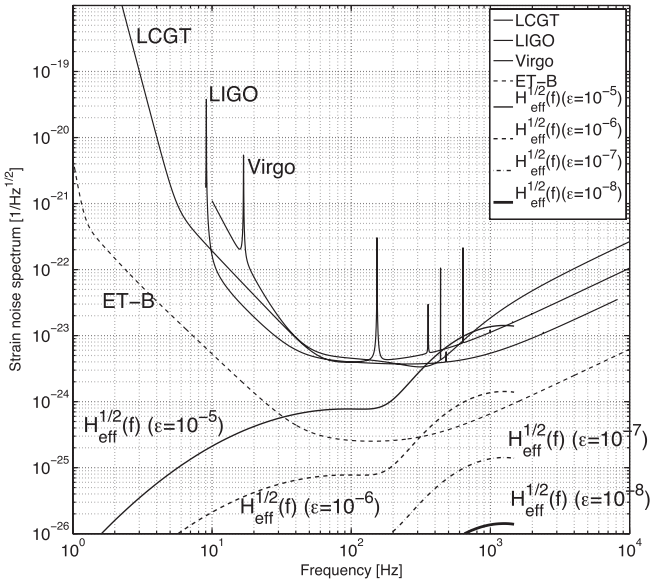

FIG. 2. One-sided noise power spectral density of LCGT, advanced LIGO, advanced Virgo, and Einstein Telescope (ET-B). LCGT noise curve is "variable RSE in broadband mode" (VRSE(B)) [27]. Advanced LIGO noise curve is "Zero Det, High Power" taken from [28]. Advanced Virgo noise curve is take from the Virgo website [29]. The Einstein Telescope noise curve is called "ET-B" [30]. The effective source power $H^{1/2}_{\rm eff}(f)$ is also plotted. In this plot, we assume $T_{\rm obs} = 1$ yr and $\langle\Gamma^2\rangle^{1/2}_{\rm 1day} = 0.2$.

TABLE II. The signal-to-noise ratio $\rho_{(V)1\ \rm yr}$ for the Virgo cluster which can be obtained with 1 year observation time for each combination of the detectors' noise PSD and $\langle\Gamma^2_{(V)}\rangle^{(1/2)}_{\rm 1day}$ given in in Table I. $\varepsilon = 10^{-5}$ is assumed. Noise PSD of AIGO is assumed to be the same as that of LIGO noise PSD. The location and the orientation of ET are assumed to be the same as those of Virgo.

$\rho_{(V)1\ \rm yr}$	LIGO-L	LIGO-H	Virgo	LCGT	AIGO	ET
LIGO-L	14.4	11.3	3.54	3.36	13.2	74.4
LIGO-H	···	11.0	2.63	3.21	9.12	55.4
Virgo	···	···	2.95	1.90	3.51	48.0
LCGT	···	···	···	3.54	3.84	37.4
AIGO	···	···	···	···	14.3	73.9
ET	···	···	···	···	···	939

is known about the location and the orientation of Einstein Telescope, we assume that it is the same as that of the Virgo detector. In practice this will certainly not be the case. However, here we perform the computations for such a hypothetical case.

From Tables I and II, we find that in the case of $\varepsilon = 10^{-5}$ we can achieve $\rho = 3$ in less than a month for the two LIGOs assuming advanced LIGO noise PSD. For one of the advanced LIGOs and LCGT, it takes about 10 months to achieve the same SNR. The LIGO detector at Louisiana and AIGO seems to work the best among advanced detectors. Assuming advanced LIGO noise PSD this baseline can achieve the target SNR in less than 20 days. If one of the detector is Einstein Telescope, it will be quite easy to observe it. However, the results strongly depend on the value of ϵ since $\rho \propto \varepsilon^2$ and $T_{\rm obs} \propto \varepsilon^{-4}$. If $\varepsilon = 10^{-6}$, it will become difficult to observe the Virgo cluster hot spot with advanced LIGO, advanced Virgo and LCGT. Only when both the detectors have sensitivity as that of the Einstein Telescope, it will be possible to detect the Virgo hot spot within a year.

The results improve if we employ several baselines of a network of detectors. A full treatment of multibaseline gravitational wave radiometry has been given in [20]. The results of this paper can be easily applied to the case of the hot spot where the source consists of a single pixel or at most a few pixels. In this case the beam matrix for a single baseline essentially consists of a single diagonal term for a single pixel or in case of few pixels, a small block diagonal matrix having dominant diagonal terms. The ρ which we have defined above is then just the SNR obtained for the log likelihood statistic λ defined in that paper. We also deduce from further results of that paper on sensitivity that approximately in our case,

$$\rho^2_{\rm network} = \sum_I \rho^2_I, \tag{26}$$

where $\rho_{\rm network}$ is the SNR for the network and the index I runs over all the baselines of the network. Similarly, it is easy from the foregoing to deduce that the observation times to reach an SNR of 3, namely $T^{\rho=3}_{\rm obs}$, add harmonically; more specifically we have,

$$\frac{1}{T^{\rho=3}_{\rm obs}} = \sum_I \frac{1}{T^{\rho_I=3}_{\rm obs}}, \tag{27}$$

where now the $T^{\rho=3}_{\rm obs}$ denotes the time of observation required for the network and $T^{\rho_I=3}_{\rm obs}$ denotes the observation time required for the baseline I to reach the SNR of 3.

We can now apply these results to various networks. We consider only the detector networks of the immediate future. The results are given in Table IV. We first consider the 3 detectors, LIGO-Virgo (L-H-V) network. Just comparing Tables II and IV, the $\rho_{(V)1\ \rm yr}$ goes up from 11.3 for two LIGOs to 12.1 for the L-H-V network which is about 7% increase. Note that one must here take into account 3 baselines: L-H, L-V and H-V. The $T^{\rho=3}_{(V)\rm obs}$ comes down from 25.8 days for the two LIGOs to 22.4 days for the L-H-V network which is a decrease of 13%. If one considers the two LIGOs along with the LCGT the improvement is almost similar to Virgo case, that is, the observation time comes down to 22.1 days. The improvement of adding other baselines to the L-H baseline is marginal because the L-H contribution is dominant. Note however that an interesting improvement is obtained if one considers a detector at AIGO site assuming same noise PSD as the LIGOs.

TABLE III. Observation time $T^{\rho=3}_{\rm obs}$ required to achieve $\rho = 3$ for each combination of the noise PSD and $\langle \Gamma^2_{(V)} \rangle^{(1/2)}_{\rm 1day}$ in Table I for the Virgo cluster. $\varepsilon = 10^{-5}$ is assumed. Noise PSD of AIGO is assumed to be the same as that of LIGO noise PSD. The location and the orientation of ET are assumed to be the same as those of Virgo.

$T^{\rho=3}_{(V)\rm obs}$ [day]	LIGO-L	LIGO-H	Virgo	LCGT	AIGO	ET
LIGO-L	15.8	25.8	262	291	18.9	0.594
LIGO-H	···	27.0	474	319	39.5	1.07
Virgo	···	···	377	907	266	1.43
LCGT	···	···	···	262	223	2.35
AIGO	···	···	···	···	16.0	0.602
ET	···	···	···	···	···	0.00372

TABLE IV. The signal-to-noise ratio $\rho_{(V)1\ \rm yr}$ which can be obtained with 1 year observation time and the observation time required to achieve $\rho = 3$ by more than 2 detectors for the Virgo cluster. These are derived from Eqs. (26) and (27) and Tables II and III. L: LIGO-Livingston, H: LIGO-Hanford, V: Virgo, J: LCGT in Japan, A: a detector with LIGO's noise PSD at the AIGO site in Australia.

Detector combination	$\rho_{(V)1\ \rm yr}$	$T^{\rho=3}_{(V)\rm obs}$ [day]
L-H-V	12.1	22.4
L-H-J	12.2	22.1
L-H-A	19.6	8.55
L-V-J	5.24	120
L-V-A	14.1	16.5
L-J-A	14.1	16.4
H-V-J	4.57	157
L-V-A	10.1	32.1
L-J-A	10.4	30.3
V-J-A	5.54	107
L-H-V-J	13.1	19.1
L-H-V-A	20.4	7.90
L-H-J-A	20.5	7.81
L-V-J-A	15.1	14.4
H-V-J-A	11.5	25.0
L-H-V-J-A	21.4	7.21

In such a L-H-A network, L-A contribution becomes dominant because of largest $\langle \Gamma^2_{(V)} \rangle^{(1/2)}_{1\text{day}}$ in Table I, and $\rho_{(V)1\ \text{yr}}$ goes up to 19.6 and $T^{\rho=3}_{(V)\text{obs}}$ comes down to 8.5 days. L-V-A and L-J-A networks are similar and give the second largest value of $\rho_{(V)1\ \text{yr}}$ among 3 detector networks. They are better than L-H-V and L-H-J cases.

In the case of a 4 or 5 detector network, we can have further improvement, but the effect is not so large since the L-H-A contribution dominates ρ. For the 4 detector case, the L-H-J-A network gives the largest value of $\rho_{(V)1\ \text{yr}} = 20.5$. The L-H-V-A network also gives similar results. In the case of the 5 detector network, $\rho_{(V)1\ \text{yr}} = 21.4$ and $T^{\rho=3}_{(V)\text{obs}} = 7.21$ days.

V. SUMMARY AND DISCUSSION

In this article we address the question of observing a hot spot of stochastic GWs using the cross-correlation statistic. The idea is to restrict the statistic to a single or few pixels in the sky and target possible point stochastic sources. A possible source which we pick is the Virgo cluster which could be a rich bed of rotating neutron stars containing an estimated number of 10^{11}. Out of these the rotating neutron stars emitting GW which fall into the bandwidth of the advanced detectors are primarily the millisecond neutron stars. We assume that the distribution of such neutron stars follows a bimodal distribution similar to that of the radio pulsars observed in our galaxy. We then see that with advanced detectors the observation time required to accumulate SNR $\sim$3 is about an order of an year if the average ellipticity of neutron stars is $\varepsilon \sim 10^{-5}$. Several baselines have been considered as well as multiple baselines corresponding to networks of detectors. In these calculations, the baselines that stand out are the two LIGO detectors and the LIGO Livingston and a LIGO-like detector at the AIGO site in Australia. These baselines have the best sensitivity, because for these baselines, the detectors are almost coaligned. In such cases, the observation time required to achieve SNR $\sim$3 is about 20 days if we assume $\varepsilon = 10^{-5}$. The future proposed Einstein Telescope can easily detect the hot spot.

However, the ellipticity of 10^{-5} might be too large from various points of view. The maximum ellipticity supportable by shear stress of neutron stars is estimated to be $10^{-6} - 10^{-7}$ (see, e.g., [21–24]) for conventional neutron stars, and 10^{-4} for neutron stars with exotic equations of state [21]. Thus, in order to realize $\varepsilon = 10^{-5}$, exotic materials may need to play a role. Regardless of the maximum ellipticity supportable, it is unclear how much ellipticity millisecond pulsars have. Cutler [25] considered internal toroidal magnetic fields as a cause of ellipticity, and claimed that millisecond pulsars may have $\epsilon = 10^{-8} \sim 10^{-9}$. The analysis of the 5th science run of LIGO has already set upper limits on the ellipticity of pulsars in our Galaxy [24]. In fact from Table I of [24], we obtain the average upper limit of $\varepsilon \lesssim 1.63 \times 10^{-6}$ for pulsars having rotation frequencies greater than 100 Hz. Further, by assuming that the observed spin-down of pulsars is due to the quadrupole emission of gravitational waves, we obtain the upper limit on ϵ. For observed millisecond pulsars in the ATNF pulsar database, the average of this upper limit becomes $\sim 10^{-8}$. If all of the millisecond pulsars which are not observed now also have such ellipticity, it will not be possible for near future advanced LIGO, advanced Virgo and LCGT to detect the hot spot. The Einstein Telescope would be able to observe the Virgo cluster hot spot if the average ellipticity is around 10^{-6}. In which case, one Einstein Telescope will be sufficient to detect the Virgo cluster by cross-correlating with other detectors like the LIGOs, Virgo and LCGT. If ε is much smaller than 10^{-6}, then it would not be very easy to detect the Virgo cluster hot spot. In such a case, if we assume a detection threshold of $\rho = 3$, and there is no detection, then an upper limit can be set on the ellipticity ε and/or the number of millisecond pulsars N_{msp} in the Virgo cluster. Inverting Eq. (24) and choosing $\hat{\mathbf{\Omega}}$ in the direction of the Virgo cluster, we have

$$\left(\frac{\varepsilon}{10^{-5}}\right)\left(\frac{N_{\text{msp}}}{4\times 10^7}\right)^{1/2} \lesssim \left(\frac{3}{\rho_{(V)1\ \text{yr}}}\right)^{1/2}\left(\frac{T_{\text{obs}}}{1\ \text{yr}}\right)^{-1/4} \times \left(\frac{I}{1.1\times 10^{45}\ \text{gcm}^2}\right)^{-1}. \quad (28)$$

Looking at Table II, for the pair LIGO-L and ET, the highest SNR is obtained, $\rho_{(V)1\ \text{yr}} \sim 75$. This pair produces the best upper limits. Assuming $N_{\text{msp}} \sim 4 \times 10^7$ the upper limit on the average ellipticity turns out to be $\varepsilon \lesssim 2 \times 10^{-6}$, which is almost the same as the current upper limit by LIGO. We should note, however, that the upper limit from the hot spot observation limits all of the pulsars in the observational frequency range which is different from the current limit on the individual pulsars. Similarly, assuming a given ellipticity will put an upper limit on the number of millisecond pulsars in the Virgo cluster. These limits will be useful for shedding light on the population and the ellipticity distribution of pulsars in the galaxies other than the Milky Way, even if the hot spot is not detected.

Although we have treated the Virgo cluster as a point source, the angular size of the Virgo cluster is about 8 degrees which is larger than the angular resolution in the current analysis, $\sim$5 degrees. This means that the signal is spread over few pixels in the sky. Thus, the SNR evaluated in this paper must be understood as a collection of SNRs spread over few pixels. In this case, the distribution of elliptical galaxies among other galaxies will affect the distribution of SNR over the pixels. Given this general scenario, the number of pulsars we have assumed per galaxy is a very rough estimate. Clearly, it is not directly proportional to the number of galaxies because of the

different sizes of the galaxies involved. A more accurate estimate would be obtained from the blue light luminosity of galaxies as is done in [26]. The actual frequency distribution of pulsars in the Virgo cluster galaxies may also be different from what we have assumed in our paper because of the observational selection effects. We believe that the rough estimate of the pulsar population in this paper is good enough for the evaluation of the feasibility of the detection of the hot spot. But we must revise these assumptions if we wish to evaluate the SNR more accurately. We propose to consider these issues in the future.

Besides the Virgo cluster, there could be other candidates for hot spots such as the Andromeda galaxy or our own galactic center. Although in these cases, the number of sources contributing to the GW background may be smaller than the Virgo cluster, their distances are much smaller, which makes up for the overall strength of the stochastic sources. We also plan to investigate these sources in our future work.

ACKNOWLEDGMENTS

S. Dhurandhar thanks S. Bose and S. Mitra for useful discussions on multiple baselines. We thank F. Takahara and S. J. Tanaka for useful discussions on the population of neutron stars. S. Dhurandhar also acknowledges the DST and JSPS Indo-Japan international cooperative program for scientists and engineers for supporting visits to Osaka City University, Japan and Osaka University, Japan. H. Tagoshi, N. Kanda and H. Takahashi thank JSPS and DST under the same Indo-Japan program for their visit to IUCAA, Pune, India. H. Tagoshi's work was also supported in part by a Monbu Kagakusho Grant-in-aid for Scientific Research of Japan (Nos. 20540271 and 23540309). N. Kanda's work was also supported in part by a Monbu Kagakusho Grant-in-aid for Scientific Research of Japan (No. 23540346). H. Takahashi's work was also supported in part by a Monbu Kagakusho Grant-in-aid for Scientific Research of Japan (No. 23740207).

[1] A. Abramovici, W. E. Althouse, R. W. P. Drever, Y. Gürsel, S. Kanwamura, F. J. Raab, D. Shoemaker, L. Sievers, R. E. Spero, K. S. Thorne, R. E. Vogt, R. Weiss, S. E. Whitcomb, and Z. E. Zucker, Science **256**, 325 (1992); C. Bradaschia *et al.*, Nucl. Instum. Methods Phys. Res. A **289**, 518 (1990); K. Danzmann *et al.*, in *First Edoardo Amaldi Conference on Gravitational Wave Experiments*, edited by E. Coccia, G. Pizzella, and F. Ronga (World Scientific, Singapore, 1995); K. Tsubono, in *Gravitational Wave Experiments*, edited by E. Coccia, G. Pizzella, and F. Ronga (World Scientific, World Scientific, Singapore, 1995).

[2] K. Kuroda, Classical Quantum Gravity **23**, S215 (2006).

[3] B. S. Sathyaprakash and B. F. Schutz, Living Rev. Relativity **12**, 2 (2009).

[4] N. Christensen, Phys. Rev. D **46**, 5250 (1992).

[5] E. E. Flanagan, Phys. Rev. D **48**, 2389 (1993).

[6] B. Allen, in *Proceedings of The Les Houches School on Astrophysical Sources of Gravitational Waves*, edited by J. A. Marck and J. P. Lasota (Cambridge University Press, Cambridge, England, 1997), p. 373.

[7] B. Allen and J. D. Romano, Phys. Rev. D **59**, 102001 (1999).

[8] B. Allen and A. C. Ottewill, Phys. Rev. D **56**, 545 (1997).

[9] H. Kudoh and A. Taruya, Phys. Rev. D **71**, 024025 (2005); A. Taruya and H. Kudoh, Phys. Rev. D **72**, 104015 (2005); H. Kudoh, A. Taruya, T. Hiramatsu, and Y. Himemoto, Phys. Rev. D **73**, 064006 (2006); A. Taruya, Phys. Rev. D **74**, 104022 (2006).

[10] S. Mitra, S. V. Dhurandhar, T. Souradeep, A. Lazzarini, V. Mandic, S. Bose, and S. Ballmer, Phys. Rev. D **77**, 042002 (2008).

[11] P. Jaranowski, A. Krolak, and B. F. Schutz, Phys. Rev. D **58**, 063001 (1998).

[12] D. R. Lorimer *et al.*, Astrophys. J. **439**, 933 (1995).

[13] D. R. Lorimer, Living Rev. Relativity **11**, 8 (2008).

[14] D. HaiLang and L. XiangDong, arXiv:0907.2507.

[15] L. Ferrario and Dayal Wickramasinghe, Mon. Not. R. Astron. Soc. **375**, 1009 (2007).

[16] S. A. Story, P. L. Gonthier, and A. K. Harding, Astrophys. J. **671**, 713 (2007).

[17] A. A. Abdo *et al.*, Astron. Astrophys. **524**, A75 (2010).

[18] F. Camilo, S. E. Thorsett, and S. R. Kulkarni, Astrophys. J. **421**, L15 (1994).

[19] ATNF Pulsar Catalogue, http://www.atnf.csiro.au/people/pulsar/psrcat/.

[20] D. Talukder, S. Mitra, and S. Bose, Phys. Rev. D **83**, 063002 (2011).

[21] B. J. Owen, Phys. Rev. Lett. **95**, 211101 (2005).

[22] C. J. Horowitz and K. Kadau, Phys. Rev. Lett. **102**, 191102 (2009).

[23] B. Abbott *et al.*, Phys. Rev. D **76**, 082001 (2007).

[24] B. P. Abbott *et al.*, Astrophys. J. **713**, 671 (2010).

[25] C. Cutler, Phys. Rev. D **66**, 084025 (2002).

[26] E. S. Phinney, Astrophys. J. Lett. **380**, L17 (1991).

[27] http://gwcenter.icrr.u-tokyo.ac.jp/en/researcher/parameter.

[28] D. Shoemaker, The LIGO Document Report No. LIGO-T0900288-v3.

[29] https://wwwcascina.virgo.infn.it/advirgo/.

[30] S. Hild, S. Chelkowski, and A. Freise, arXiv:0810.0604.